

Three-dimensional localization of MR-visible markers with potential applications in position tracking: feasibility, speed, and precision

H. Busse¹, W. Gründer², N. Garnov², M. Moche¹, and T. Kahn¹

¹Diagnostic and Interventional Radiology Dept., Leipzig University Hospital, Leipzig, Germany, ²Medical Physics and Biophysics Dept., Leipzig University, Leipzig, Germany

Introduction/Purpose

Recently, a three-dimensional (3D) marker localization technique has been shown to be feasible for automatic MR image registration during interventional procedures in a closed-bore MRI scanner [1]. That approach used inductively coupled RF micro coils as signal source and could be performed with conventional pulse sequences. Because marker detection relied on morphological processing of a fully reconstructed MR image, localization times (image acquisition and marker signal discrimination) were on the order of tens of seconds. The purpose of this work is (1) to determine whether such an approach can be adapted to be feasible for faster applications (position tracking) and (2) to thoroughly determine the corresponding reliability and spatial precision in an experimental setup.

Materials and Methods

Design, pros/cons, and applications of inductively-coupled RF micro coils (μ C) as MR markers have been described previously (e.g., [1-3]). The μ Cs used here were wound around a tube with a (short-T1) glyceroltrinitrate liquid and tuned to the resonance frequency (63.8 MHz) of a 1.5T MRI (Siemens Magnetom Symphony). Three μ Cs were mounted on a flexible MR-compatible arm (Invivo Germany GmbH, Schwerin) attached to the scanner table (Fig. 1) and were scanned in 15 arbitrary positions at different distances (d_{iso}) from the magnet isocenter and different angular orientations ($\pm\theta$, with respect to the transverse plane). A bottle of doped water served as background phantom. A balanced SSFP (TrueFISP) sequence with a square 300-mm FOV and a slice thickness of 200 mm was used. Parameters for high (HSR: matrix MX=512, partial Fourier PF=100%, pixel band width PBW=220 Hz, TR/TE=3651/2.85 ms) and low spatial resolution (LSR: MX=128, PF=50%, PBW=1565 Hz, TR/TE=254.4/1.15 ms) were used. Measurements were performed at two low flip angles (FA=1° and 2°) and two phase encode directions (PED=with and without swap) and all acquisitions were performed twice (MM=1 and 2). The marker localization determined the 3D position by matching the fitted 2D Gaussian peak positions of orthogonal acquisitions in the three standard views VW=sag, cor, and tra. The number of peaks detected in these views is denoted as {s,c,t}. In comparison with HSR, only a few 2D peak discrimination parameters had to be adapted for LSR (128²) localization.

Acquisition Acronym	Matrix Part. Fourier	PED	FA [°]	# of cases with 3 (4) markers	mean 3D localization time [ms] measured on 1.7 GHz P4	estimated* for 4-Core CPU
HSR_N_1°	512 ² - 100%	N	1	30 (0)	2265 ± 335	453 ± 67
HSR_N_2°	...	N	2	30 (0)	2614 ± 472	523 ± 94
HSR_S_1°	...	S	1	28 (2)	1712 ± 166	342 ± 33
HSR_S_2°	...	S	2	29 (1)	1966 ± 300	393 ± 60
				117 (3)	2139 ± 474	428 ± 95
LSR_N_1°	128 ² - 50%	N	1	29 (1)	448 ± 128	90 ± 26
LSR_N_2°	...	N	2	30 (0)	580 ± 211	116 ± 42
LSR_S_1°	...	S	1	30 (0)	344 ± 84	69 ± 17
LSR_S_2°	...	S	2	30 (0)	399 ± 91	80 ± 18
				119 (1)	443 ± 163	89 ± 33

* by assuming the localization to be sped up by a typical factor of 5 (see CPU chart in [5])

Tab. 1: Parameters and localization results for high and low spatial resolution (see text).

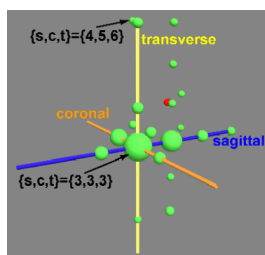


Fig. 2: Distribution of actual number of detected peaks per 2D view {s,c,t} for fast LSR acquisition (red: case with one false extra marker). Volume of spheres scales with number of cases (n=120).

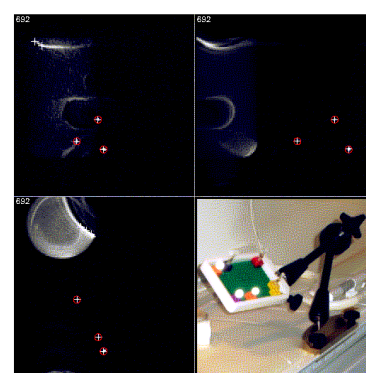


Fig. 1: Subsecond LSR marker detection. Despite {s,c,t}={4,5,6}, exactly 3 markers were localized. Inset shows flexible arm with marker plate.

Results For 45 marker positions, d_{iso} ranged from 96 to 274 mm and θ from -48° to $+65^\circ$. The detection rate for exactly 3 markers was 97.5% (HSR) and 99.2% (LSR) despite the relatively "broad" distribution of the actual number of detected peaks in each view (Fig. 2: LSR, HSR similar). The remaining cases simply involved one (false) extra peak caused by TrueFISP dispersion artifacts [4]. Neither signal contributions from the doped water nor signal reception with the body coil posed a problem. Differences in marker positions between repeated measurements (MM) showed no bias for any factor (FA, PED, VW) and averaged 0.0 ± 0.1 mm (HSR) and 0.0 ± 0.3 mm (LSR) over all 1D coordinates (n=180). Mean 3D offsets between the individual 3D coordinates and their average over FA, PED, and MM yielded 0.4 ± 0.4 mm (HSR) and 0.6 ± 0.5 mm (LSR). The average 3D distances $d_{LSR-HSR}$ between the measured 3D positions yielded mean \pm SD of only 0.95 ± 0.54 mm. This value is much smaller than the pixel-based estimate of $\sqrt{3} \cdot (\text{pixel spacing}) = 4.1$ mm. The LSR localization times for a state-of-the art PC [5] were estimated to be much smaller (<100 ms) than the underlying time for MR image acquisition, here ~ 760 ms.

Discussion and Conclusion

The presented marker localization technique is considered highly reproducible and highly reliable even at large distances from the isocenter or in tilted coil positions. The relatively small mean deviation of <1.0 mm between LSR and HSR is attributed to the fact that 2D Gaussian fitting (2D-GF) uses the signal information from several pixels to determine the peak position at subpixel resolution. In previous work, 3D marker localization based on 2D-GF in three fully reconstructed MR images was considered to be unfeasible for tracking applications. By using a smaller matrix size and half-Fourier techniques, however, acquisition times as low as 500-800 msec (for three views) will allow subsecond 3D marker localizations, especially with state-of-the art CPUs. For selected applications, such as the tracking of patient positions (motion) or interventional instruments/devices, that do not require real-time position updates, the presented technique provides a relatively simple, flexible, and safe alternative to more complex techniques. For that purpose, however, the localization algorithm needs to be part of the image reconstruction on the MR host.

References

- [1] Busse H et al., JMRI 2007;26:1087-1096, [2] Quick HH et al., MRM 2005;53:446-455, [3] Burl M et al., MRM 1996;36:491-493, [4] Wildermuth S et al., Cardiovasc Intervent Radiol 1998;21:404-410, [5] <http://www.cs.virginia.edu/stream/peecee/MFLOPS.html>.

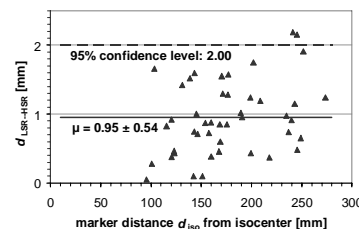


Fig. 3: Plot of mean 3D distance $d_{LSR-HSR}$ between measured LSR and HSR marker positions vs. d_{iso} .